Dielectric Behavior of Three Phase Polyimide Percolative Nanocomposites

Naga Gopi Devaraju, Burtrand I. Lee

School of Materials Science and Engineering, Clemson University, Clemson, South Carolina 29634

Received 26 April 2005; accepted 6 August 2005
DOI 10.1002/app.22856
Published online 11 January 2006 in Wiley InterScience (www.interscience.wiley.com).

ABSTRACT: Three phase ceramic–metal–plastic (cermetplas) percolative nanocomposite films were prepared using polyimide, as the matrix to prepare the composite films. Silver nanoparticles with a mean particle size of about 41 nm were prepared and used as the metal phase. Nanocomposites of barium titanate ($BaTiO_3$) particles in polyimide matrix, with silver as metallic inclusion, were formulated using effective medium theory and percolation theory. The concentration and frequency dependence of dielectric permittivity (ε) and loss tangent (tan δ) measurements were reported and discussed for cermetplas below the percolation threshold. Experimental results for cermetplas show that a ε of above 500 can be achieved below the percolation. © 2006 Wiley Periodicals, Inc. J Appl Polym Sci 99: 3018–3022, 2006

Key words: dielectric properties; nanocomposites; polyimides; silver nanoparticles; percolation

INTRODUCTION

Polymer–ceramic composites have drawn great interest recently as thick film dielectric composite materials, because of their ease of processability. There has been extensive research on these ceramic-filled dielectric composites by many research groups.[1–6] Dielectric permittivity (ε) values >100 have been achieved earlier, at high ceramic loadings of above 85 vol %. At this amount of filler, there will be little flexibility and plastic properties left in the film. The ε values that can be achieved by this is limited, even though the ε of the filler used is above 1000. Besides, the dielectric losses increase as a result of the increasing porosity of these highly loaded films. The growing need for high ε materials makes it obvious that increasing the ceramic loading in the polymer itself will not help in achieving the ever increasing needs. On the other hand, there have been reports of high $\varepsilon > 3500$ in metal–ceramic composites, but they need to be sintered at high temperatures of >1200°C.[7–9]

In this study, we report high ε, three-phase nanocomposites in the form of a film. Nanoparticles of silver (Ag) have been introduced into the optimized polymer–ceramic matrix. The formulation for these composites was based on the effective ε prediction equations[10–13] and the percolation theory.[10] If insulated from the electrodes, metal particles can be polarized in the same way as dielectric ceramics. In this case, the polarization is caused by the electron charges rather than ions. Several researchers have found experimental evidence of an increase in the ε of the composite in the neighborhood of the percolation threshold.[9,10,14–17] A very high ε value can be obtained at a conductive filler loading close to, but not exceeding, the percolation threshold. This behavior can be visualized as many conducting particles separated by thin insulating layers of polymer,[18] which may be viewed as microcapacitors.

There has been growing interest in the study and application of nanoparticles because of their unique physical properties exhibited at such small sizes, with high surface area. In our study, nanoparticles of silver have been used, with an aim of forming a large number of such interfacial/microcapacitors to achieve higher dielectric constants. These nano particles were synthesized with a surfactant layer to control the size and the dispersion. Polyimide has been chosen as the matrix because of its better toughness, chemical and thermal stability, and lower coefficient of thermal expansion (CTE) than epoxy.

EXPERIMENTAL

Silver particles were prepared in a method similar to that reported earlier.[19,20] Silver ions from silver nitrate was reduced by sodium borohydride (SBH). A mixture of mercaptosuccinic acid (thiol ligand) and lauric acid (acid ligand) was used as the surfactants to control the size and disperse the silver particles produced. $AgNO_3$ in precalculated amount was dissolved in about 2 mL of water and was mixed with a solution of

Correspondence to: B. I. Lee (Lburtra@clemson.edu).

thiol and acid ligands in anhydrous methanol of about 10 times that of water. The mole ratio of thiol to acid ligands was kept at 1 : 4.5 and that of thiol to silver at 2 : 1. Freshly prepared SBH solution was added to the silver solution dropwise under stirring, and allowed for 10 min for the reduction reaction to be completed. This solution is then refluxed in anhydrous methanol three times to remove the extra organic and inorganic ions. All these chemicals were obtained from Aldrich, and were used in between as received condition. 3,3′,4,4′-benzophenone tetracarboxylic dianhydride (BTDA) [98% purity] and 4,4′-oxydianiline (ODA) [97% purity] were obtained in polymer grade purity from Aldrich and were used as the monomers for polyimide (PI) without further purification. *N*-methyl-2-pyrrolidinone (NMP) [99+, A.C.S. reagent] obtained from Aldrich was distilled and used as the solvent. Distillation was carried out to minimize the absorbed water content in the solvent. Hydrothermal $BaTiO_3$ (BT-08 from Cabot Performance Materials, Boyertown, PA) was used as the ceramic filler having an average particle size of 240 nm. BYK-W9010 a copolymer with acidic groups (flash point > 100°C) having a moisture content of about 0.02% was obtained from Byk-Chemie, Germany, and used as the dispersant for $BaTiO_3$.

PI was synthesized via poly(amic acid) (PAA) route. A 100 mL round bottom flask, equipped with a mechanical stirrer is set up in a glove box attached with a continuous N_2 inlet and drying tube containing calcium sulfate. ODA of 0.016 mol in 12 mL of NMP was placed in the round bottom flask. The solution was stirred until all the diamine was dissolved. The same molar content, i.e., 0.016 mol of BTDA in 12 mL of NMP was added, as a subsequent step. The mixture of diamine and dianhydride in dipolar aprotic solvent, NMP, was stirred at room temperature in N_2 atmosphere for 24 h to yield a clear, viscous, yellow-brown solution of PAA. The solution was used for the preparation of films that were subsequently cyclized thermally into final PI. The overall process flow diagram is given in Figure 1.

The dispersant BYK-W9010 (2 wt % of $BaTiO_3$) was dissolved in NMP and ceramic powder was then introduced into this NMP, followed by ball milling for 15 h. The weight ratio of the solvent to ceramic was maintained at 1 : 2. Precalculated amounts of $BaTiO_3$ (the ball milled slurry) and PAA mixture were stirred magnetically for 2 h and ultrasonicated for 15 min. A homogeneous sol of $BaTiO_3$/PAA was obtained. This sol, in predetermined proportions, was added to the silver nanoparticles and homogenized by stirring magnetically for half an hour and degassed in vacuum for 30 min before being cast. The mixed sol was then cast on a clean, dry indium tin oxide (ITO) glass substrate by spin coating at a speed of 1500 rpm for 30 s. Good adhesion was obtained on the ITO glass substrates for both the base PAA–$BaTiO_3$ composite sols as well as the PAA–$BaTiO_3$–Ag sols.

The intermediate PAA is converted to PI by thermal imidization with the optimized thermal cycle to achieve close to 100% imidization of the PAA. The heating cycle followed was 100°C for 1 h (in vacuum), 200°C for 1 h, and 300°C for 2 h, followed by slow cooling to room temperature. Single layer thick films of ~5 μm were obtained after thermal curing.

Room temperature XRD (RTXRD, Scintag PAD V using Cu Kα with λ = 0.15406 nm) was used for crystalline phase identification of the samples with step scan mode: step 0.02°, 5 s/step, 2 = 20–80°: 40 kV, 40 mA. Thickness and surface roughness measurements were performed with a noncontact surface profilometer with 1.5×, 20×, and 100× magnification heads (Topo-3D, 2D by Wyko Corp.) with a vertical scanning range of 1 nm–500 μm. Surface morphology of PI–$BaTiO_3$ films after coating with platinum was observed by using cold field emission scanning electron microscopy (Hitachi Cold Field Emission FE SEM 4700).

RESULTS AND DISCUSSION

The curing behavior of the PI and PI–$BaTiO_3$ composites has been reported earlier in our previous paper. The resulting composite was stable upto 300°C. XRD patterns revealed that there are no secondary impurity phases present, resulting from the fabrication process of the composite capacitor.[21]

The volume fraction of $BaTiO_3$ for the formulation of cermetplas was optimized and that composition was used for further investigation of percolation dielectric composite properties. Figure 2 shows the ε of the two phase PI–$BaTiO_3$ composite films at 100 kHz. The ε of the composite increases with the volume of filler expectedly. Figure 2 also shows the calculated values from several well-known models/equations, as follows.

Maxwell-Garett approximation[10,11]:

$$\varepsilon = 1 + \frac{3f_{BaTiO_3}\beta}{1 - f_{BaTiO_3}\beta} \tag{1}$$

Bruggerman self-consistent effective medium approximation[10,12]:

$$\varepsilon = (1 - f_{BaTiO_3})\frac{\varepsilon_1 - \varepsilon}{\varepsilon_1 + 2\varepsilon} + f_{BaTiO_3}\frac{\varepsilon_2 - \varepsilon}{\varepsilon_2 + 2\varepsilon} \tag{2}$$

and Jayasundere and Smith model[13]:

$$\varepsilon = \frac{\varepsilon_1 f_{PI} + \varepsilon_2 f_{BaTiO_3}[3\varepsilon_1/(\varepsilon_2 + 2\varepsilon_1)] \times [1 + 3f_{BaTiO_3}(\varepsilon_2 - \varepsilon_1)]}{\varepsilon_1 f_{PI} + \varepsilon_2 f_{BaTiO_3}[3\varepsilon_1/(\varepsilon_2 + 2\varepsilon_1)][1 + 3f_{BaTiO_3}(\varepsilon_2 - \varepsilon_1)]} \tag{3}$$

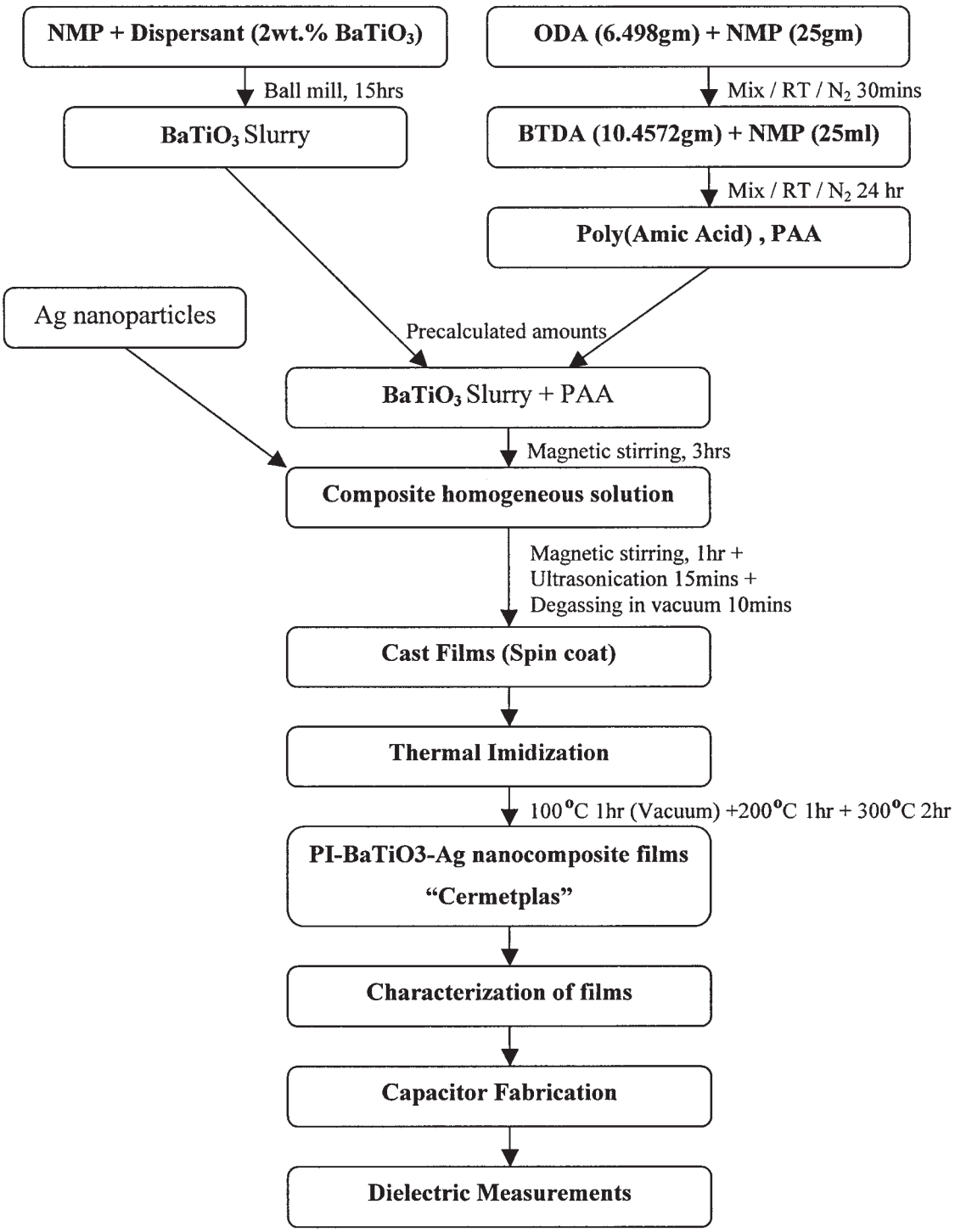

Figure 1 Flow diagram for the fabrication of thick film three phase capacitors.

where $\beta = (\varepsilon_2 - \varepsilon_1)/(\varepsilon_2 + 2\varepsilon_1)$; ε is the ε of the $BaTiO_3$/PI composite; $\varepsilon_1 = 3.5$ and $\varepsilon_2 = 1400$ are used as the dielectric constants of the PI matrix and the $BaTiO_3$ ceramic particles, respectively. f_{BaTiO3} is the volume fraction of $BaTiO_3$, and f_{PI} is the volume fraction of PI in the composite.

As seen from Figure 2, the experimental results are in agreement with those calculated by eqs. (1), (2), and (3) up to $f_{BaTiO3} \sim 0.3$. At $f_{BaTiO3} = 0.3$, the ε of the composite reaches about 5–6 times that of the PI matrix. At higher volume fractions, the experimental results start to deviate from the calculated values. This deviation in the ε from the predicted or calculated values may be because of the increased porosity as the higher ceramic loading increased. This porosity can be confirmed by the SEM micrograph shown in Figure 3

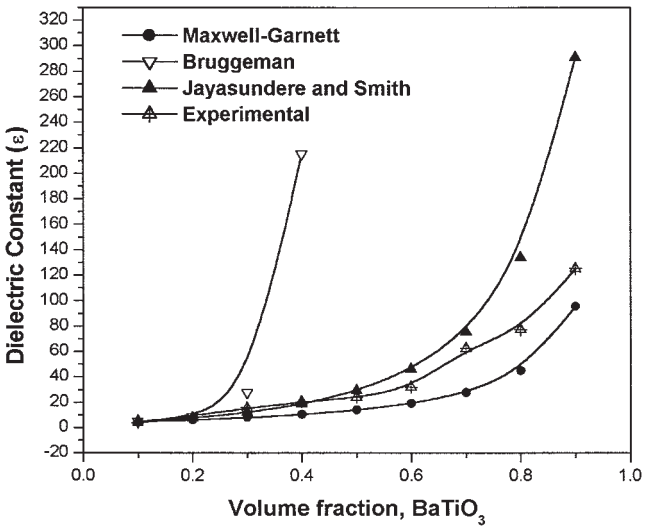

Figure 2 Variation of ε of the $BaTiO_3$/PI composites for different volume fractions of $BaTiO_3$ at 100 kHz.

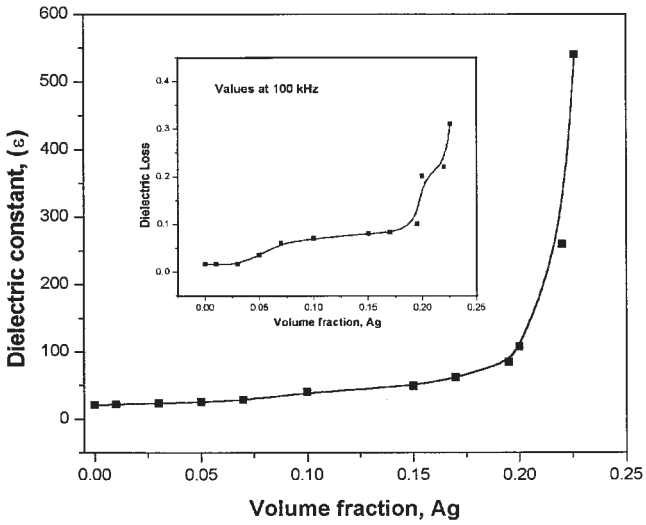

Figure 4 Variation of effective ε of the three phase cermetplas percolative composite, with increasing volume fraction of silver. Dielectric loss values were given in the inset.

for a composite of $f_{BaTiO3} = 0.4$. For this reason, the volume fraction of $BaTiO_3$ was chosen as 0.3 for further investigations.

Silver nanoparticles synthesized were incorporated into the PI–$BaTiO_3$ composite matrix in increasing amounts of volume fraction. The ε of the three phase composites were enhanced by applying the percolation phenomenon. Figure 4 shows the dielectric behavior of the PI–$BaTiO_3$–Ag three phase composites. The increase in the ε was small until the metal particle concentration became close to the percolation threshold. This is explained by the power law[8]:

$$\varepsilon = \varepsilon_o |(f_c - f_{Ag})/f_c|^{-q} \quad (4)$$

where ε_0 is the ε of the base PI–$BaTiO_3$ composite with $f_{BaTiO3} = 0.3$. f_c is the percolation threshold volume fraction of Ag, and f_{Ag} is the volume fraction of silver in the composite. The experimental values of the ε are in good agreement with the eq. (4), with $f_c = 0.23$ and $q = 0.8$. A ε value of above 500 was achieved at 100 kHz with a dielectric loss of 0.23 at Ag filler content of 0.22. An important interesting note here is a ε of $\sim$1500 can be achieved by f_{Ag} nearer to f_c threshold of the composite. The dielectric loss of the composites increased proportional to the ε, as shown in Figure 4. As the material gets more conducting, ε increases as does the frequency dispersion. The ε increases due to space charge build up at the interfaces between the conducting and the insulating phases because of the difference in conductivity of the two phases.[22] In addition at higher loadings of conducting phase, the contribution to ε from the space charge at the metal polymer interface would diminish as the frequency increases, this explains the lower values of ε at higher frequencies. Similar results have been reported by Dang et al.[23] with ε value of $\sim$800 at a loss of 0.5 at 100 Hz. Although the dielectric loss, tan δ, was $>$0.32 near the percolation threshold, there may some applications because of its high dielectric constant.[23]

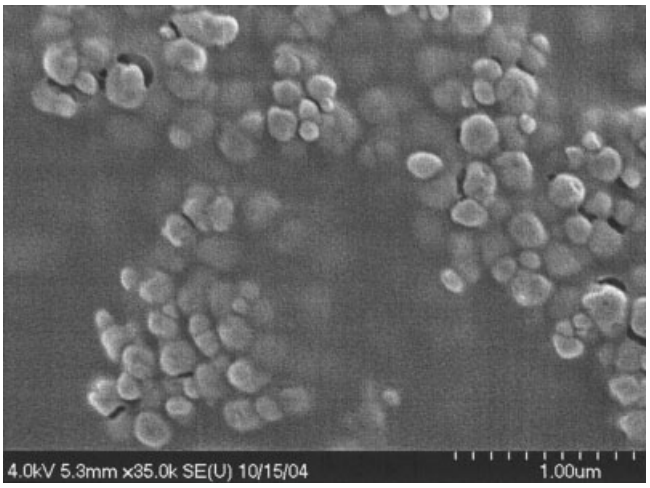

Figure 3 SEM micrograph of 40 vol % $BaTiO_3$ in polyimide matrix.

The frequency dependence of the composites was very weak at low filler volume contents. However, the composites containing Ag particles close to the threshold (22 vol %) exhibit a stronger frequency dependence of ε, as shown in Figure 5. The higher ε exhibited in this case can be explained by the formation of a large number of small capacitors, formed by particles with very thin dielectric layers.[18,24]

CONCLUSIONS

Composite thick films were developed with PI matrix-containing $BaTiO_3$ particles in optimized amount

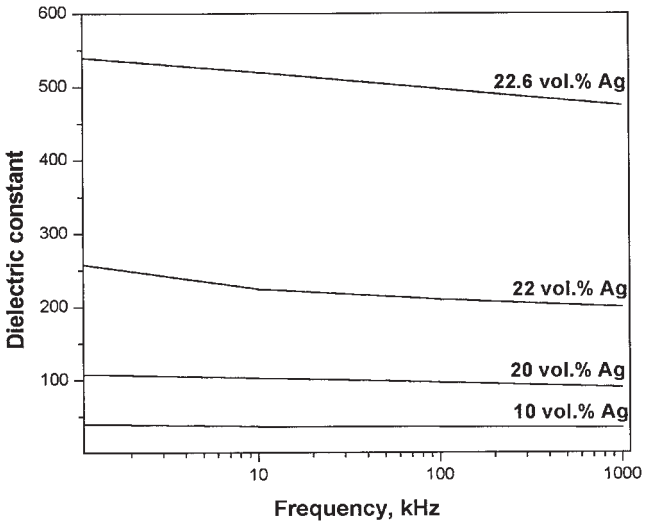

Figure 5 ε variation with frequency for various volume contents of Ag filler.

along with various amounts of silver nanoparticles. The dependence of ε on the frequency and the conducting filler content were studied. The ε of the composites can be enhanced greatly by introducing metal particles in it. Processing ease and flexibility to make thick film capacitors, and high dielectric constant, make them candidates for a wide variety of energy storage applications.

References

1. Hitesh, W.; Markondeya, R. P.; Balaraman, D.; Bhattacharya, S. K.; Tummala, R. IEEE Trans Electron Packag Manuf 2003, 26, 2.
2. Rao, Y.; Takahashi, A.; Wong, C. P. Compos A 2003, 34, 1113.
3. Andresakis, J.; Yamamoto, T.; Biunno, N. Circ World 2003, 30, 36.
4. Ogitani, S.; Bidstrup, A. S.; Kohl, P. Presented at the IPC conference, San Diego, April 2–6, 2000.
5. Cho, S. D.; Lee, J. Y.; Paik, K. W. Electron Compon Technol Conf 2002, 504.
6. Manish, N.; Jeanine, A. C.; Lawrence, S., Jr.; Sen, A. Chem Mater 1991, 3, 201.
7. Halder, N.; Das, S. A.; Khan, S. K.; Sen, A.; Maiti, H. S. Mater Res Bull 1999, 34, 545.
8. Chen, R.; Wang, X.; Gui, Z.; Ti, L. J Am Ceram Soc 2003, 86, 1022.
9. Pecharroman, C.; Moya, J. S. Adv Mater 2000, 12, 294.
10. Nan, C. W. Prog Mater Sci 1993, 37, 1.
11. Nan, C. W. Phys Rev B 2001, 63, 176201.
12. Bruggeman, D. A. G. Ann Phys (Leipzig) 1935, 24, 636.
13. Jayasundere, N.; Smith, B. V. J Appl Phys 1995, 34, 6149.
14. Pecharroman, C.; Esteban, B. F.; Moya, J. S. Adv Mater 2001, 13, 1541.
15. Wu, J. J.; McLachlan, D. S. Phys Rev B 1997, 56, 1236.
16. Wu, J. J.; McLachlan, D. S. Phys Rev B 1998, 58, 14880.
17. Brosseau, C. J Appl Phys 2002, 91, 3197.
18. Kuzel, R.; Krivka, I.; Kubat, J.; Prokes, J.; Nespurek, S.; Klason, C. Synthetic Met 1994, 67, 255.
19. Jana, N. R.; Peng, X. G. J Am Chem Soc 2003, 125, 14280.
20. Chen, S. H.; Kimura, K. Langmuir 1999, 15, 1075.
21. Devaraju, N. G.; Lee, B. I. Microelectron Eng 2005, 82, 71.
22. VonHippel, A. R. Dielectrics and Waves; Wiley: New York, 1953.
23. Dang, Z.-M.; Shen, Y.; Nan, C.-W. Appl Phys Lett 2002, 81, 4814.
24. Qi, L.; Lee, B. I. Adv Mater 2005, 17, 1777.